Dalton Transactions

Accepted Manuscript

ROYAL SOCIETY OF CHEMISTRY

www.rsc.org/dalton

Journal Name

ARTICLE

Ultra-small Mesoporous Silica Nanoparticle as an Efficient Carrier for pH Responsive Releases of Anti-cancer Drugs

Received 00th January 20xx,
Accepted 00th January 20xx

DOI: 10.1039/x0xx00000x

www.rsc.org/

Haoquan Zheng*, Cheuk-Wai Tai, Jie Su, Xiaodong Zou, Feifei Gao*

Mesoporous silica has emerged as one of the most promising carriers for drug delivery system. However, the synthesis of ultra-small mesoporous silica nanoparticle (UMSN) and its application in drug delivery remains a significant challenge. Here, spherical UMSNs (~ 25 nm) have been synthesized and tested as drug carriers. Anti-cancer drugs mitoxantrone (MX), doxorubicin (DOX) and methotrexate (MTX) have been utilized as model drugs. The pH-responsive drug delivery system can be constructed based on electrostatic interaction between carriers and drug molecules. The UMSNs could store drugs under the physiological condition while releases them under acidic conditions. Different pH-responsive release profiles were obtained in phosphate buffer solutions (PBSs) under designed pH values (from 4.0 to 7.4). MX and DOX can be used in pH-responsive delivery system, while MTX cannot be used. Furthermore, we found that the physiological stabilities of these drug molecules in UMSNs are in a decreasing order MX > DOX > MTX, which follows the order of their isoelectric point (pI) values.

Introduction

Anti-cancer drugs mitoxantrone (MX) and doxorubicin (DOX) are anthracenedione antineoplastic agents that intercalate with DNA and exert potent immunomodulating effects suppressing humoral immunity.[1, 2] Although they have shown positive therapeutic effects, they may cause side effects because they disrupt the DNA synthesis and DNA repair in both healthy cells and cancer cells. Other anti-cancer drugs, such as the antifolate therapeutic agent methotrexate (MTX), also face a similar problem.[3, 4] Thus, "smart" drug delivery systems, which can store or release drug molecules in response to external stimuli including pH,[5-14] light,[15] temperature,[16] chemical reactions[17] and enzymes,[18] are used in the pharmaceutical industry to directionally release drugs and reduce side effects.[19, 20] Amongst these, "smart" drug delivery systems based on pH variations have been extensively studied. For instance, the pH difference between stomach (pH 1.2) and intestine (pH 6.8 – 7.4) was used to build pH triggered systems for oral drug delivery. Furthermore, the pH targeting approach is regarded as a more feasible strategy than many other targeting approaches for anti-cancer drugs, since tumour extracellular microenvironments, endosomal and lysosomal compartments are more acidic than blood and normal tissues.[21] Thus, it is important to design a pH-responsive delivery system for typical anti-cancer drugs, such as MX, DOX and MTX.[22, 23]

Carriers in the drug delivery systems potentially influence both loading and releasing processes. Therefore developing efficient and economical carriers is very important in the research on drug delivery systems, in particular achieving practical applications in pharmacy. Polymers, hydrogels, micelles, liposomes and inorganic solids have been reported as carriers in pH-responsive drug delivery systems.[7, 24, 25] However unsatisfactory stability in physiological environment limits the effective applications of polymers and hydrogels.

Mesoporous silica has emerged as one of the most promising carriers owing to their good biocompatibility, high surface area, large pore volume, tuneable pore sizes, facile synthesis routes, and capability to load and release various drugs via their mesopores.[26-39] In a very recent report,

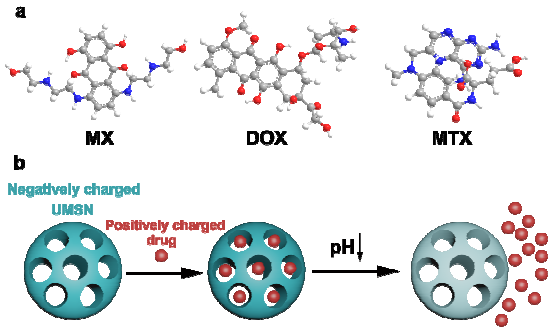

Scheme 1. a) Molecular structural models of anti-cancer drugs (nitrogen atoms are shown in blue, oxygen in red, carbon in grey, and hydrogen in white); b) Schematic mechanism for the pH-responsive delivery system using UMSN as a carrier.

[a] *Berzelii Center EXSELENT on Porous Materials and Department of Materials and Environmental Chemistry, Stockholm University, Stockholm, SE-106 91(Sweden)*
† Corresponding authors: feifei.gao@mmk.su.se, haoquan.zheng@mmk.su.se
Electronic Supplementary Information (ESI) available: [The solubilization kinetic profiles of free drugs, porosity properties, wide angle XRD patterns and stability test of drug loaded UMSN]. See DOI: 10.1039/x0xx00000x

mesoporous silica nanoparticles were developed for cancer-targeted drug delivery in vivo after functionalization.[40] pH–responsive systems based on mesoporous silica materials usually involve on/off capping or gating (by functional groups,[41, 42] polyelectrolyte[43-46] and ring–shaped compounds[7, 8, 47-49]) or host–guest interactions (electrostatic [50, 51], covalent bonding [52, 53] and coordination bonding[10, 54, 55]). The preparations of the pH responsive systems in large-scale are often very costly due to the complex processes. In order to increase consequent adsorption and conjugation of molecules, the surface of mesoporous silica materials should be modified by additional functional groups in most cases, which might be a potential risk in further applications in pharmaceutical industry. Therefore, simple fabrications of pH-responsive drug delivery systems by using non-functionalized mesoporous silica materials are of ultimate interests.

In order to obtain efficient and economical drug delivery systems, mesoporous silica nanoparticles (MSNs) are preferred to construct a simple drug delivery system via direct host-guest interactions between MSNs and drug molecules, although there might be a size-dependent toxicity in a certain case.[56] Ultra-small mesoporous silica nanoparticles (UMSNs) have more advantages over the conventional MSNs because the decrease of their particle sizes to nanometres shortens the access path of drug molecules, increases drug loading/releasing rate, and enhances interactions between the carrier and drug molecules during loading.[57] In addition, UMSNs will be concentrated in the tumour tissues due to the enhanced permeability and retention (EPR) effect caused by small particle size and imported into the cancer cells via pinocytosis and phagocytosis.[58, 59]

As well known, it still remains challenging in controlling the morphology, porosity, and in particularly the dispersion of small mesoporous particles. [60-62] This is an obstacle for the migration of drug molecules since UMSNs usually cause an aggregation. Recently, we have developed a novel technique to synthesize well dispersed UMSNs. UMSNs with ca. 25 nm in size were synthesized by using a time-controlled sequence of dilution and pH quenching. The pH adjustments were introduced to avoid aggregation of UMSNs and stabilize the colloidal suspension. The change in final pH values of the pH adjustments would give rise to various stabilization conditions of UMSN.

Here we show that these UMSNs can be used as the carriers to construct an efficient and economical pH-responsive drug delivery system for the anti-cancer drugs mitoxantrone (MX) and doxorubicin (DOX) without the need of post-functionalization of UMSNs. Furthermore, we investigated the working mechanism of this pH-responsive delivery system and proposed a criterion for selecting possible drug molecules to be used in this system. The pH-responsive release from MX or DOX-loaded UMSNs demonstrated their potential to be applied in tissue specific delivery systems for anti-cancer drugs.

Materials and Methods

Materials and characterizations

The following reagents were purchased and used without further purification: NaOH (Sigma–Aldrich), HCl (37 %, Sigma–Aldrich), NaCl (Sigma–Aldrich), PBS at various pHs (Sigma–Aldrich), cetyltrimethylammonium bromide (CTAB, Sigma–Aldrich), Pluronic F127 ($EO_{106}PO_{70}EO_{106}$, Sigma–Aldrich), tetraethyl orthosilicate (TEOS, Sigma–Aldrich), MX (Sigma–Aldrich), DOX (Yinghuan Chempharm) and MTX (Yinghuan Chempharm).

Powder X-ray diffraction (PXRD) patterns were collected on a PANalytical X'Pert Pro diffractometer equipped with a Pixel detector using Cu Kα1 (λ = 1.5406 Å) radiation. High-resolution transmission electron microscopy (HRTEM) images were taken on a JEOL JEM-2000FXII microscope operated at 200 kV. The UMSNs were dispersed in PBS (pH 7.4) to determine the size distribution and zeta potential of the nanoparticles by dynamic light scattering **(**DLS, Malvern Zetasizer Nano Series). Conductivities of MX, DOX and MTX were measured by HI 98312 DiST®1 TDS Tester at different pH values. N_2 sorption isotherms were recorded at 77 K on a Micromeritics ASAP2020 analyser.

Synthesis of UMSNs

Typically, 0.2 g of CTAB and 0.003 g of F127 were dissolved in a mixture of 2.3 g NaOH solution (1 M) and 8.78 g deionized H_2O. Then, 1 ml of TEOS was added. After a short time stirring (40 s), 75 ml of deionized water was used to dilute the above solution. After 4 min, 1.1 ml of HCl solution (2 M) was applied to adjust the pH value to 5.5, followed by stirring for 3 h, and then 0.6 g of NaOH solution (1 M) was added. The reaction mixture was stirred for another 1 h and aged at room temperature for 2 days under static conditions. The precipitate was collected by centrifugal separation and washed at least three times with a mixture of ethanol and H_2O. The powder product was dried at 60 ^{o}C overnight. Surfactants were removed by calcination at 550 ^{o}C for 6 h.

Measurement of isoelectric point (pI)

To obtain a drug solution, 5 ml of stock solutions of drug was added to 50 ml of NaCl solution (1 mM), then successive amount of NaOH solution (0.1 M) was added to achieve pH 11.5. The pH value was then adjusted from 11.5 to a predetermined set down to pH 3. The conductivities of these drug solutions (denoted as $Cond_{drug}$) under various pH conditions were measured by a conductivity meter. The conductivities of a blank experiment with only NaCl solution (1 mM) under various pH conditions were denoted as $Cond_{blank}$. At a certain pH, standard conductivity of drug in NaCl solution (denoted as △Cond) was calculated by the following formula: $\triangle Cond = Cond_{drug} - Cond_{blank}$. The pI of each drug molecule can be determined by the pH value, at which the conductivity reaches the minimum.

Loading of anti-cancer drug in the mesopores of the UMSNs

The loadings of the three drugs MX, DOX and MTX in UMSNs followed the same procedure. Then 0.05 g UMSNs were added into 10 ml drug solution with the concentration of 200 μg/ml at a designed pH and stirred at room temperature for 24 h.

The products were obtained by centrifugation and washed for three times with PBS at pH 7.4.

Release of anti-cancer drug from UMSNs in PBS solution

Taking MX release experiments as an example, the release system was prepared by suspending 10 mg MX-loaded UMSN material into 20.0 ml PBS by vibration with different pH values from 4.0 to 7.4 at 37 ^{o}C. In the case of sampling, 1 ml of the homogenous solution was withdrew and centrifuged, followed by being measured with UV-Vis spectrophotometer. The release of DOX or MTX followed the same process as that of MX. The amount of released guest molecules was measured by UV–Vis spectrophotometer. The release percentage of the drug (MX, DOX or MTX) was calculated according to the following formula: release percentage (%) = m_r / m_l, where m_r is the amount of released drug while m_l is the total amount of loaded drug.

Results and Discussions

UMSNs as Drug Carriers

The UMSNs were synthesized using CTAB as a structure directing agent (SDA), neutral surfactant F127 as a particle stabilization agent and TEOS as a silica source. To obtain monodispersed UMSNs, pH adjustments were necessary to avoid particle agglomerate and also to stabilize the colloidal suspension. After removal of CTAB, UMSNs were obtained. HRTEM image and SEM image show that the UMSNs have spherical shape with an average size of 25 nm and ordered mesostructures (Fig. 1a and ESI Fig. S1). These UMSNs are highly dispersed with narrow size distributions in both deionized water (20 – 30 nm) and phosphate buffer solutions (PBSs) (25 – 40 nm), as indicated by DLS (Fig. 1b). The particle sizes in PBS are slightly larger than those in deionized water, which can be explained by the solvation layers of sodium ions or potassium ions attached to the surface of the UMSNs in PBS. The PXRD pattern of the UMSNs shows only one peak at 1.25 ^{o} with a d-spacing of 7.0 nm (Fig. 1c), which indicates the presence of some degrees of ordering of the mesopores in these ultra-small nanoparticles. N_2 sorption shows a typical type IV isotherm with a surface area of 452 m^2 g^{-1} and an average pore diameter of 4 nm (ESI Fig. S2).

For a pH-responsive drug delivery system based on electrostatic interactions, the charges of the drug carrier should be changed with the peripheral pH. The isoelectric point (pI) value of a carrier is defined as the pH value at which

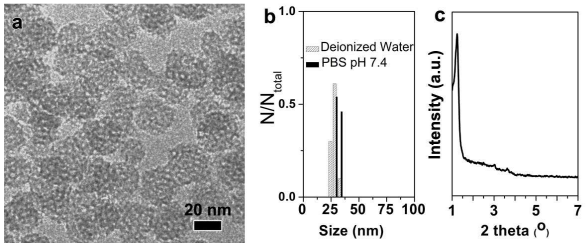

Fig. 1. TEM images (a), size distribution determined by DLS (b) and PXRD pattern (c) of UMSNs.

the carrier has zero net charge. To determine the pI value and quantify the charges of the UMSNs, laser electrophoresis zeta-potential measurement was employed. The zeta potential of a carrier reflects the charge of the carrier, which is zero at the isoelectric point. The pI value of the UMSNs is ca. 3.0 as obtained from zeta potential plot (Fig. 2). The zeta potential decreases quickly from 0.1 mV at pH 3.0 to -36.5 mV at pH 6.0, then slowly falls to -39.8 mV at pH 7.0, and finally keeps almost constant at pH above 8.0. [51] This indicates that the UMSNs are negatively charged above pH 3 due to the large amount of negatively charged silanol groups on the surface of UMSNs, and the negative charge increases with pH.

Anti-cancer Drug Molecules

Anti-cancer drugs are mostly small organic molecules with multi-functional groups. These organic molecules can activate or inhibit the function of biomolecules, which in turn results in therapeutic benefits to patients. To construct an efficient drug

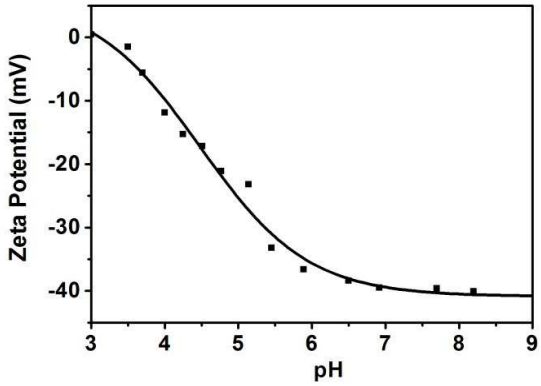

Fig. 2. Plot of zeta potentials of UMSNs at different pH values.

delivery system via UMSNs, the drug molecules should be smaller than the mesopores (4 nm) so that they can access the inner surface of the UMSNs rather than only load on the external surface of the particles. We chose three commonly used anti-cancer drugs, MX, DOX and MTX as the test drugs, with the molecule sizes of about 1.2 × 2.0 × 0.3 nm, 1.0 × 1.5 × 0.3 nm and 1.0 × 1.8 × 0.3 nm, respectively (Scheme 1a), obtained by measuring the distances between the two outermost atoms and taking into account the Van der Waals radii of the atoms.

With multi-functional groups in the molecules, MX, DOX and MTX contain both acidic and basic functional groups. For example, the phenolic hydroxyl groups in both MX and DOX molecules and the carboxyl groups in MTX can be negatively charged, while ethanolamine groups and aniline groups in MX and amine groups in DOX and MTX can be positively charged. These drug molecules thus are positively or negatively charged by gaining or losing protons, depending on pH values. To investigate the electrostatic interaction between the UMSN carrier and a drug, it is important to determine the pI value of the drug molecule. The relationship between the pI values of a drug molecule and peripheral pH is: (i) when pH > pI, the drug molecule is negatively charged; (ii) when pH ≈ pI, the drug

molecules are neutral; and (iii) when pH < pI, the drug molecule is positively charged, and a drug delivery system can be constructed on the drug via the electrostatic attraction between the negative charges of UMSNs and the positive charges of the drug molecules.

We applied one of the widely used methods to determine the pI value of a drug molecule, which is based on the measurement of conductivity change of the drug solution compared to the drug-free solution at different pH values.[63] NaCl solution (1 mM) was used to prepare the drug solution. The pH values were achieved by adding successive amounts of NaOH solution to the drug solution. The conductivities of MX, DOX and MTX were measured at different pH values and shown in Fig. 3. The pI value of each drug molecule corresponds to the pH value where the conductivity reaches the minimum, i.e. 9.5 for MX, 8.2 for DOX and 5.4 for MTX. It should be noted that the pI values of MX and DOX are higher than pH 7.4, indicating that MX and DOX molecules are positively charged under physiological condition (pH 7.4). At pH 7.4, MX or DOX molecules can be stored at in the mesopores of the UMNSs due to electrostatic interaction, while it is difficult to store MTX molecules due to the repulsions between negatively charged silanol groups and MTX molecules.

Loading of Drug Molecules in UMSNs via Electrostatic Interaction

In order to construct pH-responsive drug delivery systems, different interactions between drug molecules and carriers are required at different pH values. The interaction can be illustrated by a simple experiment measuring the amount of drugs loaded in the mesopores of UMSNs via electrostatic interactions under various pH conditions (Fig. 4). As shown in Fig. 4a, the loading amount of MX increased from 12 mg/g at pH 4.0 to 283 mg/g at pH 9.0, indicating that the attraction between UMSNs and MX increased with pH. Although a larger loading amount of MX was obtained under stronger alkali conditions, a large amount of drug molecules would release at PBS (pH 7.4). For DOX molecules (Fig. 4b), there was an obvious increase of drug loading from pH 4.0 to 7.0. However, the loading amount decreased with a further increase of the pH, which is caused by the loss of positive charges from DOX when pH is close to or above its pI value (8.2). The result of loading amount vs pH in the MTX delivery system suggests a more complicated interaction between UMSNs and MTX molecules (Fig. 4c). The strength of electrostatic interactions at pH 4.0 and 5.0 is very weak due to the small amount of net charges given by both negatively charged UMSNs and positively charged MTX. When the pH is above 5.0, repulsive forces exist between UMSNs and MTX, which leads to a decrease in the loading amount with the increase of pH. The loading of MTX under these conditions is then driven by physical adsorption.

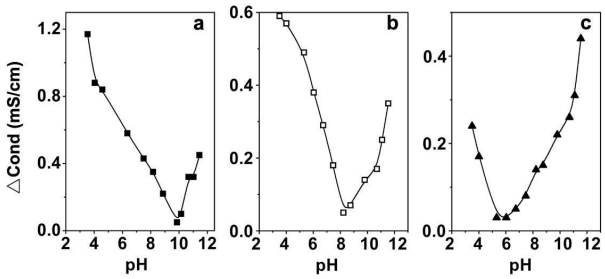

Fig. 3. Standard conductivities of MX (a), DOX (b) and MTX (c) in NaCl solution (1 mM) at different pH values.

Notably, the solubility of drug molecules at a given pH is also influenced by pI value, thus tests for the influence of drug solubility on pH-responsive releases were performed. The amounts of drugs in these tests were the same as those in UMSNs at pH 7.4. The solubilizations of drugs in all profiles are approximately 100 % within one hour (ESI Fig. S3). Therefore, the solubility did not contribute to the pH-responsive releases of MX, DOX and MTX from UMSNs.

Loading and *In-vitro* pH-responsive Release of Drug Molecules

The change of interactions between the drug molecules and the UMNSs with pH leads to either loading or releasing of the drugs. The profiles of pH-responsive release of MX, DOX and MTX from UMSNs in acidic conditions are shown in Fig. 5. There is a rapid release in the first five hours, then no significant release is observed after 5 h. The release is only about 12% at pH 7.4 and 13% at pH 6.0 for MX, owing to the stable electrostatic attraction under the physiological condition. However, the release of MX (Fig. 5a) is 34% at pH 5.0, due to the weaker electrostatic attraction at lower pH. When DOX is used in this system, the release amount of DOX is 11% at pH 7.4. Under weakly acidic conditions, the release of DOX is 63% at pH 6.0, and 79% at pH 5.0 (Fig. 5b). These results indicate a safe storage of MX and DOX under physiological conditions, and an increased amount of release with the decrease of pH (Scheme 1). Thus, a designed pH-responsive release system for anti-cancer drug MX and DOX is successfully achieved via UMSN carriers.

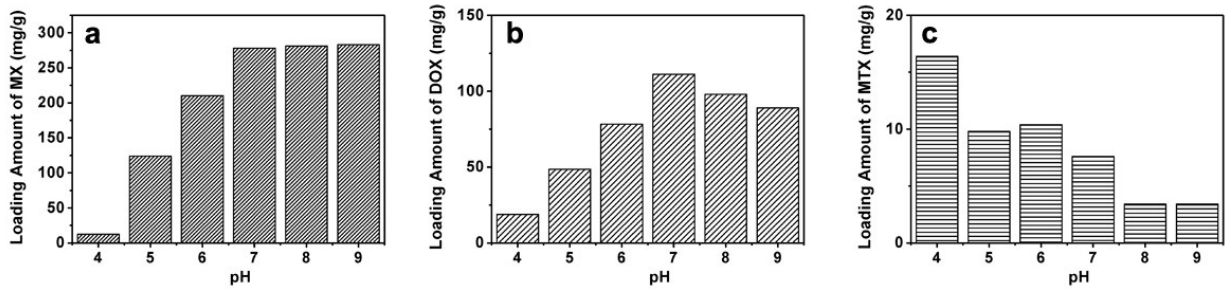

Fig. 4. The loading amounts of MX (a), DOX (b) and MTX (c) in UMSNs at different pH values.

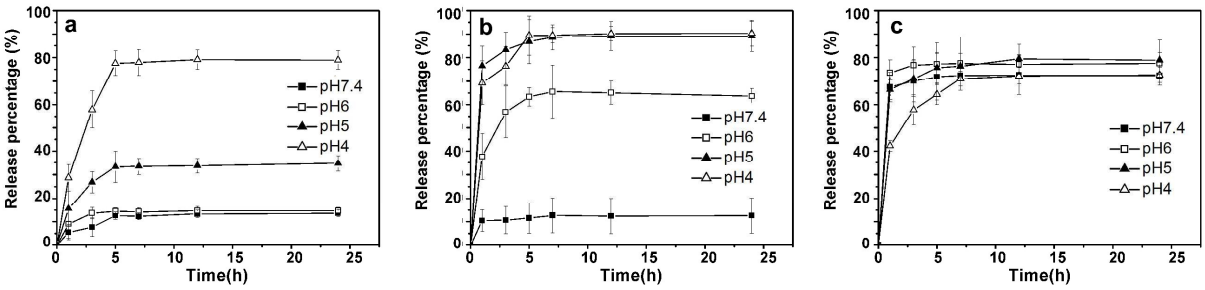

Fig. 5. The release profiles of MX (a), DOX (b) and MTX (c) from UMSNs at different pH values. Results in (a), (b) and (c) are presented as mean ± standard deviation (n=3).

The porosity and stability of drug-loaded UMSNs were studied by PXRD, TEM and N_2 sorption. In the case of MX, both surface area and mesopore volume of MX-loaded UMSNs are smaller than those of the UMSNs, indicating the successful loading of MX molecules in their mesopores (ESI Table S1). Wide angle PXRD of the drug loaded UMSNs was performed (ESI Fig. S4), and only one broad peak within the range of 6 - 60° (2ϑ) from the amorphous silica carriers was observed, indicating that no crystalline drug was formed. PXRD pattern (ESI Fig. S5a) and TEM image (ESI Fig. S5b) indicate that the original size and morphology of the UMSNs are remained. After being treated in PBS solution at pH 7.4 for 24 h, the MX-loaded UMSNs retained high porosity of the mesopore system. But the surface area and the pore volume decreased slightly from 333 to 317 m^2/g, and 0.50 to 0.48 cm^3/g, respectively. A small shrinkage of mesostructure could occur during the treatment in PBS solution for 24 h (ESI Table S1). A stable colloidal suspension of MX-loaded UMSNs in ESI Fig. S5c indicates a good dispersity after MX loading. The particle size ranges from 50 to 65 nm based on the DLS result (ESI Fig. S5d), which is larger than that of the UMSNs. And the zeta potential of the drug-loaded UMSNs decreases to -31.5 mV. Therefore, the increase of particle size can be attributed to the agglomeration of the UMSNs caused by the loss of negative charges of the UMSNs after loading positively charged drugs.

A significant release (higher than 70 %) of MTX within 7 h is observed at pH 7.4 in Fig. 5c. This fast release can be explained by the weak interaction between UMSNs and MTX molecules in which both attraction and repulsion are negligible. MTX via UMSNs as a carrier is difficult to achieve at a pH condition of human digestion system. Nevertheless, the results from MTX-loaded UMSNs could be useful in developing a criterion for suitable drug molecules for the drug delivery system with non-functionalized UMSNs.

Conclusions

In conclusion, ultra-small mesoporous silica nanoparticles (UMSNs) with ca 25 nm in size have been successfully synthesized and utilized as carriers for drug delivery without the need for further functionalization. A controllable pH-response drug release system has been designed, based on the electrostatic attraction between negatively charged silanol groups and positively charged drug molecules. The physiological stability of these drug molecules in UMSNs follows the same order as their pI values. MX and DOX, whose pI values are 9.5 and 8.2 respectively, are successfully employed in the delivery system via UMSNs as the carrier owing to the strong attractions between the drug molecules and the UMSNs. On the contrary, MTX has a relatively low pI value (5.4), which was too low in a pH-responsive drug delivery system using UMSNs as the carrier. The drug delivery system using UMSNs as carriers provides a new and efficient route for pH-responsive drug delivery applications, especially for anti-cancer therapy, with improved site specificity and release kinetics to accommodate different therapeutic purposes.

Acknowledgements

We thank the financial support from VINNOVA and VR through Berzelii Center EXSELENT on Porous Materials. Dr. F. Gao thanks the VINNMER program of VINNOVA. The Knut and Alice Wallenberg Foundation is acknowledged for an equipment grant for the electron microscopy facility at Stockholm University. We thank Dr. Alfonso Garcia and Xin Xia for valuable discussions and comments.

Notes and references

1. L. S. Rosenberg, M. J. Carvlin and T. R. Krugh, *Biochemistry (Mosc).* 1986, **25**, 1002-1008.
2. J. M. Rosenholm, C. Sahlgren and M. Linden, *Nanoscale*, 2010, **2**, 1870-1883.
3. G. Edan, D. Miller, M. Clanet, C. Confavreux, O. Lyon-Caen, C. Lubetzki, B. Brochet, I. Berry, Y. Rolland, J. C. Froment, E. Cabanis, M. T. Iba-Zizen, J. M. Gandon, H. M. Lai, I. Moseley and O. Sabouraud, *J. Neurol. Neurosurg. Psychiatry*, 1997, **62**, 112-118.
4. B. S. Parker, T. Buley, B. J. Evison, S. M. Cutts, G. M. Neumann, M. N. Iskander and D. R. Phillips, *J. Biol. Chem.*, 2004, **279**, 18814-18823.
5. E. R. Gillies and J. M. J. Frechet, *Chem. Commun.*, 2003, 1640-1641.
6. M. B. Yatvin, W. Kreutz, B. A. Horwitz and M. Shinitzky, *Science*, 1980, **210**, 1253-1255.
7. T. D. Nguyen, K. C. F. Leung, M. Liong, C. D. Pentecost, J. F. Stoddart and J. I. Zink, *Org. Lett.*, 2006, **8**, 3363-3366.
8. C. Park, K. Oh, S. C. Lee and C. Kim, *Angew. Chem. Int. Ed.*, 2007, **46**, 1455-1457.
9. S.-M. Lee, H. Chen, C. M. Dettmer, T. V. O'Halloran and S. T. Nguyen, *J. Am. Chem. Soc.*, 2007, **129**, 15096-15097.
10. H. Zheng, L. Xing, Y. Cao and S. Che, *Coord. Chem. Rev.*, 2013, **257**, 1933-1944.
11. V. Cauda, C. Argyo, A. Schlossbauer and T. Bein, *J. Mater. Chem.*, 2010, **20**, 4305-4311.
12. S. Niedermayer, V. Weiss, A. Herrmann, A. Schmidt, S. Datz, K. Muller, E. Wagner, T. Bein and C. Brauchle, *Nanoscale*, 2015, **7**, 7953-7964.
13. J. Croissant, X. Cattoën, M. W. C. Man, A. Gallud, L. Raehm, P. Trens, M. Maynadier and J.-O. Durand, *Adv. Mater.*, 2014, **26**, 6174-6180.
14. J. Croissant, D. Salles, M. Maynadier, O. Mongin, V. Hugues, M. Blanchard-Desce, X. Cattoën, M. Wong Chi Man, A. Gallud, M. Garcia, M. Gary-Bobo, L. Raehm and J.-O. Durand, *Chem. Mater.*, 2014, **26**, 7214-7220.
15. T. D. Nguyen, K. C. F. Leung, M. Liong, Y. Liu, J. F. Stoddart and J. I. Zink, *Adv. Funct. Mater.*, 2007, **17**, 2101-2110.
16. C.-Y. Lai, B. G. Trewyn, D. M. Jeftinija, K. Jeftinija, S. Xu, S. Jeftinija and V. S. Y. Lin, *J. Am. Chem. Soc.*, 2003, **125**, 4451-4459.
17. X. Guo and F. C. Szoka, *Acc. Chem. Res.*, 2003, **36**, 335-341.
18. A. Schlossbauer, J. Kecht and T. Bein, *Angew. Chem. Int. Ed.*, 2009, **48**, 3092-3095.
19. P. T. Regan, J.-R. Malagelada, E. P. DiMagno, S. L. Glanzman and V. L. W. Go, *N. Engl. J. Med.*, 1977, **297**, 854-858.
20. M. J. Sailor and J.-H. Park, *Adv. Mater.*, 2012, **24**, 3779-3802.
21. K. Engin, D. B. Leeper, J. R. Cater, A. J. Thistlethwaite, L. Tupchong and J. D. McFarlane, *Int. J. Hyperther.*, 1995, **11**, 211-216.
22. M. J. Piccart-Gebhart, M. Procter, B. Leyland-Jones, A. Goldhirsch, M. Untch, I. Smith, L. Gianni, J. Baselga, R. Bell, C. Jackisch, D. Cameron, M. Dowsett, C. H. Barrios, G. Steger, C.-S. Huang, M. Andersson, M. Inbar, M. Lichinitser, I. Láng, U. Nitz, H. Iwata, C. Thomssen, C. Lohrisch, T. M. Suter, J. Rüschoff, T. Sütő, V. Greatorex, C. Ward, C. Straehle, E. McFadden, M. S. Dolci and R. D. Gelber, *New Engl. J. Med.*, 2005, **353**, 1659-1672.
23. T. A. Yap, C. P. Carden and S. B. Kaye, *Nat Rev Cancer*, 2009, **9**, 167-181.
24. P. Gupta, K. Vermani and S. Garg, *Drug Discovery Today*, 2002, **7**, 569-579.
25. Y. Qiu and K. Park, *Adv. Drug Deliv. Rev.*, 2001, **53**, 321-339.
26. M. Vallet-Regí, F. Balas and D. Arcos, *Angew. Chem. Int. Ed.*, 2007, **46**, 7548-7558.
27. M. Vallet-Regi, A. Rámila, R. P. del Real and J. Pérez-Pariente, *Chem. Mater.*, 2000, **13**, 308-311.
28. W. Xia and J. Chang, *J. Control. Release*, 2006, **110**, 522-530.
29. V. Cauda, L. Mühlstein, B. Onida and T. Bein, *Microporous Mesoporous Mater.*, 2009, **118**, 435-442.
30. I. Slowing, B. G. Trewyn and V. S. Y. Lin, *J. Am. Chem. Soc.*, 2006, **128**, 14792-14793.
31. I. I. Slowing, B. G. Trewyn, S. Giri and V. S. Y. Lin, *Adv. Funct. Mater.*, 2007, **17**, 1225-1236.
32. F. Qu, G. Zhu, S. Huang, S. Li, J. Sun, D. Zhang and S. Qiu, *Microporous Mesoporous Mater.*, 2006, **92**, 1-9.
33. C.-P. Tsai, C.-Y. Chen, Y. Hung, F.-H. Chang and C.-Y. Mou, *J. Mater. Chem.*, 2009, **19**, 5737-5743.
34. Q. He, Y. Gao, L. Zhang, Z. Zhang, F. Gao, X. Ji, Y. Li and J. Shi, *Biomaterials*, 2011, **32**, 7711-7720.
35. B. Fadeel and A. E. Garcia-Bennett, *Adv. Drug Deliv. Rev.*, 2010, **62**, 362-374.
36. F. Tang, L. Li and D. Chen, *Adv. Mater.*, 2012, **24**, 1504-1534.
37. M. Vallet-Regí and E. Ruiz-Hernández, *Adv. Mater.*, 2011, **23**, 5177-5218.
38. Y. Chen, H. Chen and J. Shi, *Adv. Mater.*, 2013, **25**, 3144-3176.
39. S. H. van Rijt, D. A. Bölükbas, C. Argyo, S. Datz, M. Lindner, O. Eickelberg, M. Königshoff, T. Bein and S. Meiners, *ACS Nano*, 2015, **9**, 2377-2389.
40. Q. Zhang, X. Wang, P.-Z. Li, K. T. Nguyen, X.-J. Wang, Z. Luo, H. Zhang, N. S. Tan and Y. Zhao, *Adv. Funct. Mater.*, 2014, **24**, 2450-2461.
41. R. Casasús, M. D. Marcos, R. Martínez-Máñez, J. V. Ros-Lis, J. Soto, L. A. Villaescusa, P. Amorós, D. Beltrán, C. Guillem and J. Latorre, *J. Am. Chem. Soc.*, 2004, **126**, 8612-8613.
42. R. Casasús, E. Climent, M. D. Marcos, R. Martínez-Máñez, F. Sancenón, J. Soto, P. Amorós, J. Cano and E. Ruiz, *J. Am. Chem. Soc.*, 2008, **130**, 1903-1917.
43. Y. Zhu, J. Shi, W. Shen, X. Dong, J. Feng, M. Ruan and Y. Li, *Angew. Chem. Int. Ed.*, 2005, **44**, 5083-5087.
44. Q. Yang, S. Wang, P. Fan, L. Wang, Y. Di, K. Lin and F.-S. Xiao, *Chem. Mater.*, 2005, **17**, 5999-6003.
45. S. W. Song, K. Hidajat and S. Kawi, *Chem. Commun.*, 2007, 4396-4398.
46. W. Xu, Q. Gao, Y. Xu, D. Wu and Y. Sun, *Mater. Res. Bull.*, 2009, **44**, 606-612.
47. K. C. F. Leung, T. D. Nguyen, J. F. Stoddart and J. I. Zink, *Chem. Mater.*, 2006, **18**, 5919-5928.
48. C. R. Thomas, D. P. Ferris, J.-H. Lee, E. Choi, M. H. Cho, E. S. Kim, J. F. Stoddart, J.-S. Shin, J. Cheon and J. I. Zink, *J. Am. Chem. Soc.*, 2010, **132**, 10623-10625.

49. V. Cauda, C. Argyo and T. Bein, *J. Mater. Chem.*, 2010, **20**, 8693-8699.
50. C.-H. Lee, L.-W. Lo, C.-Y. Mou and C.-S. Yang, *Adv. Funct. Mater.*, 2008, **18**, 3283-3292.
51. Y. Ma, L. Zhou, H. Zheng, L. Xing, C. Li, J. Cui and S. Che, *J. Mater. Chem.*, 2011, **21**, 9483-9486.
52. B. Wang, C. Xu, J. Xie, Z. Yang and S. Sun, *J. Am. Chem. Soc.*, 2008, **130**, 14436-14437.
53. A. Popat, J. Liu, G. Q. Lu and S. Z. Qiao, *J. Mater. Chem.*, 2012, **22**, 11173-11178.
54. H. Zheng, Y. Wang and S. Che, *J. Phys. Chem. C*, 2011, **115**, 16803-16813.
55. L. Xing, H. Zheng, Y. Cao and S. Che, *Adv. Mater.*, 2012, **24**, 6433-6437.
56. I. Passagne, M. Morille, M. Rousset, I. Pujalté and B. L'Azou, *Toxicology*, 2012, **299**, 112-124.
57. M. Wu, Q. Meng, Y. Chen, Y. Du, L. Zhang, Y. Li, L. Zhang and J. Shi, *Adv. Mater.*, 2015, **27**, 215-222.
58. L. Hu, Z. Mao and C. Gao, *J. Mater. Chem.*, 2009, **19**, 3108-3115.
59. H. Hatakeyama, H. Akita and H. Harashima, *Adv. Drug Deliv. Rev.*, 2011, **63**, 152-160.
60. K. Suzuki, K. Ikari and H. Imai, *J. Am. Chem. Soc.*, 2003, **126**, 462-463.
61. J. Kobler, K. Möller and T. Bein, *ACS Nano*, 2008, **2**, 791-799.
62. S. Sadasivan, C. E. Fowler, D. Khushalani and S. Mann, *Angew. Chem. Int. Ed.*, 2002, **41**, 2151-2153.
63. A. J. Sophianopoulos and E. A. Sasse, *J. Biol. Chem.*, 1965, **240**, 1864-1866.

TOC

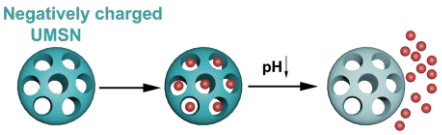

A pH-responsive drug delivery system via mesoporous silica nanoparticles as carrier can be achieved based on electrostatic interaction between drug molecules and carrier, when the isoelectric point of the drug molecule is high.